

Supporting information

Debut of enzyme-responsive anionic cyanine for overlap-free NIR-II-to-I dual-channel tumour imaging

Feiyi Chu,^a Bin Feng^a, Yiyang Zhou^a, Min Liu^{a,b}, Hailiang Zhang^a, Meihui Liu^a, Qian Chen^c, Shengwang Zhang^c, Yeshuo Ma^c, Jie Dong^a, Fei Chen^a, Wenbin Zeng^{*,a}

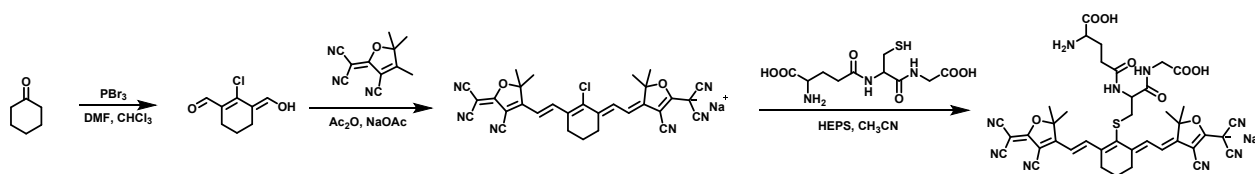
^a Xiangya School of Pharmaceutical Sciences, Central South University, Changsha, 410078, PR China.

^b Department of Pharmacy, Xiangya Hospital, Changsha 410008, PR China.

^c Third Xiangya Hospital, Central South University, Changsha 410013, PR China.

E-mail addresses: wbzeng@hotmail.com (W. Zeng); Tel/Fax: 0086-731-82650459.

1. Synthesis of compounds



Scheme S1. Synthesis of CFC-GSH.

Synthesis of Tricyanofuran

Tricyanofuran (TCF) was prepared according to the previous procedure [1].

Synthesis of CFC-Cl

TCF (958 mg, 4.81 mmol) and 2-chloro-3-(hydroxymethylene)-1-cyclohexene-carboxaldehyde (276 mg, 1.6 mmol) were suspended in acetic anhydride (15 mL), followed by the addition of sodium acetate (395 mg, 4.81 mmol). The mixture was refluxed at 150 °C for 30 min in the atmosphere of nitrogen. After that, the reaction system was cooled to room temperature, and then poured into 100 mL water. The pH was adjusted to 7.4 by the addition of sodium carbonate. Then, the precipitate was filtered and redissolved in methanol, followed by concentrated in vacuo. The residue was purified by column chromatography on silica gel (CH₂Cl₂:MeOH, 90:10, v/v) to afford a red solid (657.2 mg, 53%). ¹H NMR (600 MHz, CD₃OD) δ 8.21 (d, *J* = 14.1 Hz, 2H), 6.07 (d, *J* = 14.1 Hz, 2H), 2.61 (s, 4H), 1.88 – 1.84 (m, 2H), 1.65 (s, 12H). ¹³C NMR (151 MHz, CD₃OD) δ 176.83, 167.19,

140.04, 128.17, 115.06, 114.54, 114.17, 107.12, 95.26, 83.34, 45.17, 25.93, 25.88, 20.80.

Synthesis of CFC-GSH

GSH (552 mg, 1.8 mmol) and CFC-Cl (100 mg, 0.18 mmol) were dissolved in 20 mL DMF/HEPES buffer (1:1, v/v, 20 mM, pH = 7.4). The mixture was stirred at room temperature for 3 h in the atmosphere of nitrogen. The reaction was monitored by TLC until CFC-Cl disappeared, at which point saturated ammonium chloride solution was added. Then, the mixture was extracted with 120 mL DCM:MeOH (5:1, v/v). The combined organic layers were washed with brine, and dried over anhydrous sodium sulphate. The organic solvent was concentrated under reduced pressure to afford the crude product, and further purified by column chromatography on silica gel using MeOH as eluent to afford green pure product (111.4 mg, 77%). ¹H NMR (600 MHz, CD₃OD) δ 8.71 (d, *J* = 14.0 Hz, 2H), 6.07 (d, *J* = 14.0 Hz, 2H), 4.58 – 4.55 (m, 1H), 3.77 (t, *J* = 6.1 Hz, 1H), 3.67 (s, 2H), 3.16 (ddd, *J* = 16.3, 15.2, 8.2 Hz, 2H), 2.70 – 2.60 (m, 2H), 2.57 (t, *J* = 5.7 Hz, 4H), 2.29 – 2.12 (m, 2H), 1.86 – 1.82 (m, 2H), 1.62 (s, 12H). ¹³C NMR (151 MHz, *d*₆-DMSO) δ 176.72, 176.71, 173.22, 172.51, 169.82, 167.12, 153.33, 141.55, 134.56, 116.06, 115.17, 114.73, 107.51, 95.80, 83.17, 54.29, 53.32, 44.97, 43.13, 38.34, 31.60, 26.96, 26.94, 26.30, 21.03. HRMS: theoretical for C₄₀H₃₈N₉O₈S [M-H]⁻, 804.2570; found, 804.2573.

2. Measurement methods

Materials and apparatus

All chemicals were of analytical reagent grade and applied without further refinement. All solutions and buffers were prepared using deionized water that have been passed through a water ultra-purification system. A Bruker AV-500 spectrometer (Rheinstetten, Germany) was used to obtain the ¹H NMR spectra and ¹³C NMR spectra. High-resolution mass spectra (HRMS) were measured on a Thermo Scientific instrument. High-performance liquid chromatography (HPLC) analysis was performed on an Agilent 1100 system with a C8 column (American). A UV-2450 UV-visible spectrophotometer (Shimadzu, Japan) was used to measure the UV-vis spectra. The NIR-I fluorescence spectra were recorded using an F-7100 fluorescence spectrophotometer (Hitachi, Japan) with a voltage of 700 V. The NIR-II fluorescence spectra were collected using an FLS1000 photoluminescence spectrometer (Edinburgh Instruments, UK), while the power of the excitation light is 0.5 W. The excitation and emission slit widths were both set as 5 nm. A Leica TCS SP8 (MP+X) confocal laser scanning microscope (Leica, Germany) was employed to collect the fluorescent cell images. In vitro and in vivo NIR-I and NIR-II fluorescence imaging were performed using the Full Spectrum Animal In Vivo Imaging System AniView Phoenix 600 (Guangzhou Biolight Biotechnology Co. Ltd.).

General procedure for GGT detection

Unless otherwise noted, the fluorescence of **CFC-GSH** (5 μ M) reacting with GGT was determined in DMSO/PBS (3:7, v/v, pH 7.4). The stock solution (10 mM) of **CFC-GSH** was prepared by dissolved in DMSO. In a test tube, 955 μ L of DMSO/PBS (295 μ L + 660 μ L) and 5 μ L of the stock solution of **CFC-GSH** were mixed, followed by adding GGT solution (40 μ L, 2 U/mL in PBS). After incubation at 37 $^{\circ}$ C for 22 min on a shaker incubator, the portion of the reaction solution was transferred to a quartz cell to measure the UV–vis absorption in the range of 500–1000 nm, and fluorescence emission spectra with $\lambda_{\text{ex}} = 620/890$ nm respectively at 37 $^{\circ}$ C. At the same time, a solution containing no GGT (control) was prepared and measured under the same conditions for comparison. The error bars displayed the standard deviations from three independent assays.

Limit of detection

The detection limit was calculated based on the fluorescence titration. In the absence of GGT, the fluorescence emission spectrum of **CFC-GSH** was measured six times and the standard deviation of blank measurement was achieved. To gain the slope, the fluorescence intensity ratio (F_{660}/F_{930}) was plotted to the concentration of GGT. The detection limit was calculated with the following equation:

$$\text{Detection limit} = 3\sigma/k$$

wherein σ is the standard deviation of blank measurement, and k is the slope between the F_{660}/F_{930} versus GGT concentration.

HPLC traces for response behaviour

The probe **CFC-GSH** was incubated with GGT for 20 min at 37 $^{\circ}$ C and then the incubation system was monitored by high-performance liquid chromatography (HPLC) on an Agilent Technologies 1100 Infinity LC system. While, **CFC-GSH** was used as the reference. The mobile phases were degassed with an ultrasonic apparatus for 15 min. Mobile phase: A: water, B: methanol; elution: 0 - 3 min 65% B (isocratic), 3 - 7 min 65 - 80% B (gradient), 7 - 10 min 80% B (isocratic). Injection volume: 200 μ L; flow rate: 15.0 mL/min; detection wavelength: 365 nm.

Selectivity and competitive experiments

Potential biological interferences including 10% fetal bovine serum (FBS), 200 U/L enzymes (NTR, APN, ALP, Try, CE, GOx) and 100 μ M amino acids (Glu and Cys) and **CFC-GSH** (5 μ M) were introduced into a DMSO/PBS (3/7, v/v, 10 mM, pH = 7.4) mixed solution, and added to a black 96-well plate for 200 μ L. The fluorescence images were recorded before and after the addition of GGT (80 U/L) to the mixture for 22 min at 37 $^{\circ}$ C, around 660 nm and 1075 nm excited by 605 and 808 nm lasers, respectively.

Stock solutions (10 mM) of testing species including amino acids (Hcy, Iso, Leu, Arg, Lys and Phe) and ions (Na^+ , K^+ , Mg^{2+} , Ca^{2+} , Al^{3+} , Fe^{2+} , H_2PO_4^- , NO_3^- , CO_3^{2-}) dissolved in PBS were prepared ready, and then further diluted with a DMSO/PBS (3/7, v/v, 10 mM, pH = 7.4) mixed solution to prepare a final concentration of 100 μM and kept at 4 °C in a refrigerator. The fluorescence intensity ratio was calculated after 22 min at 37 °C, upon addition of GGT at excitation of 620 nm and 808 nm with emissions of 660 nm and 930 nm, respectively.

Cell culture and cytotoxicity test

HEK293T, Hepa 1-6, HepG2, A549, B16F10 cells were cultured in DMEM high glucose medium, and SKOV3 cells were cultured in 1640 medium, supplemented with 10% Fetal Bovine Serum (FBS), 0.2% Amphotericin B, 1% Penstrep under the environment of 37 °C incubator with 5% CO_2 . And cytotoxicity of probe **CFC-GSH** to HEK293T and HepG2 cells was performed by MTT assay. HEK293T and HepG2 cells were distributed into 96-well plates with a density of 10,000 cells per well, respectively, and incubated overnight in 37 °C incubator with the culture medium. Then 0-50 μM probes were added to the corresponding wells for 24 h, respectively. After that, the additional MTT (5 mg/mL, 20 μL) was added into each well and continued to incubate for another 4 h. Then, the liquid in the wells was discarded, and 150 μL DMSO was added to each well with shaking on a shaker for 10 min. Finally, the absorbance was taken by the microplate reader to acquire the survival rate.

Confocal fluorescence imaging

HEK293T, SKOV3, HepG2, Hepa 1-6, A549, and B16F10 cells were seeded on dishes with a cover glass bottom and allowed to adhere at 37 °C and 5 % CO_2 overnight. After washing three times with PBS, the adherent cancer cells were treated with/without acivicin (1 mM) and prepared in medium for 30 min at 37 °C in an incubator with 5 % CO_2 . Then, the living cells were incubated with **CFC-GSH** (5 μM , 0.5% DMSO) for 30 min and treated with Hoechst (1 μM) for another 5 min. The confocal fluorescence images were acquired at red channels (650–700 nm) upon excitation at 620 nm.

Homolysis assay

Fresh whole blood (2 mL) was collected from healthy female BALB/c mice. Red blood cells (RBCs) were isolated from centrifugation at 1500 rpm for 5 min, washed with PBS buffer until the supernatant was clear, and resuspended using PBS (50 mL) to prepare 4% RBCs solution. Then, different concentrations (1, 2, 4, 8, 16, 32, 64, 128, 256, and 512 μM) of **CFC-GSH** dissolved in PBS were added to the same-volume 4% RBCs solution in centrifuge tubes. A positive control was prepared by mixing 0.5 mL of ultra-pure water and 0.5 mL of the 4% RBCs solution, while a negative control consisted of 0.5 mL of PBS buffer mixed with 0.5 mL of the 4% RBCs solution. After incubation at 37 °C for 2 h, the supernatant was obtained through centrifugation at 1500 rpm for

5 min and transferred to a 96-well plate. The absorbance at 540 nm was measured by a Multiskan FC microplate photometer (Thermo). The following formula was used to calculate the homolysis percentage:

$$\text{Homolysis (\%)} = (A_{\text{sam}} - A_{\text{neg}}) / (A_{\text{pos}} - A_{\text{neg}}) \times 100$$

A_{sam} represents the absorbance of the sample, A_{neg} represents the absorbance of RBCs, A_{pos} represents the absorbance of the positive control.

In vivo toxicity assessment

BALB/c nude mice were used to evaluate the in vivo toxicity of **CFC-GSH**, which were randomly assigned into 2 groups (n = 3 per group; two groups were named PBS and **CFC-GSH**). Then, **CFC-GSH** (100 μL , 10 μM in PBS, containing 1% DMSO) was injected into the mice in two groups via the tail vein. On 24 h post-injection, the mice were sacrificed and dissected to collect major organs including the heart, liver, spleen, and kidneys, which were subsequently fixed in 4% paraformaldehyde, processed routinely into paraffin, sliced, and stained with haematoxylin and eosin (H&E). The H&E-stained slices were imaged by optical microscopy.

3. Figures

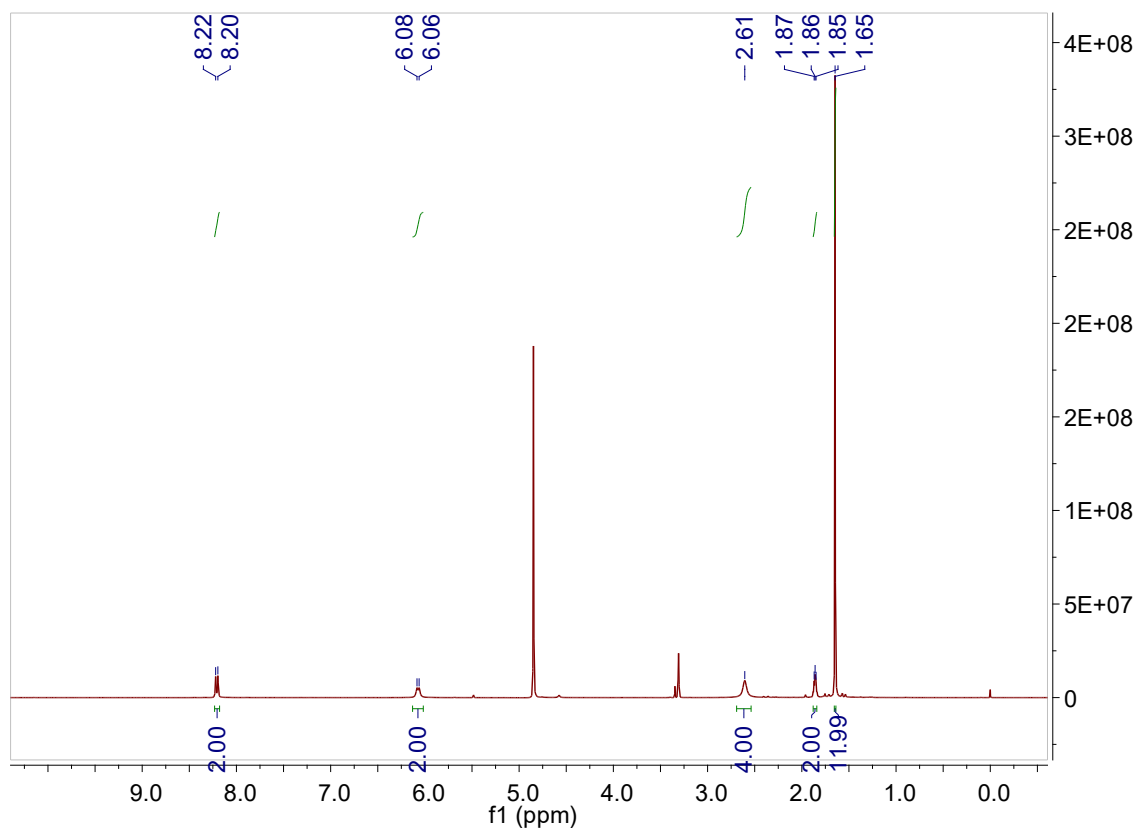


Figure S1. ^1H NMR spectrum of CFC-Cl.

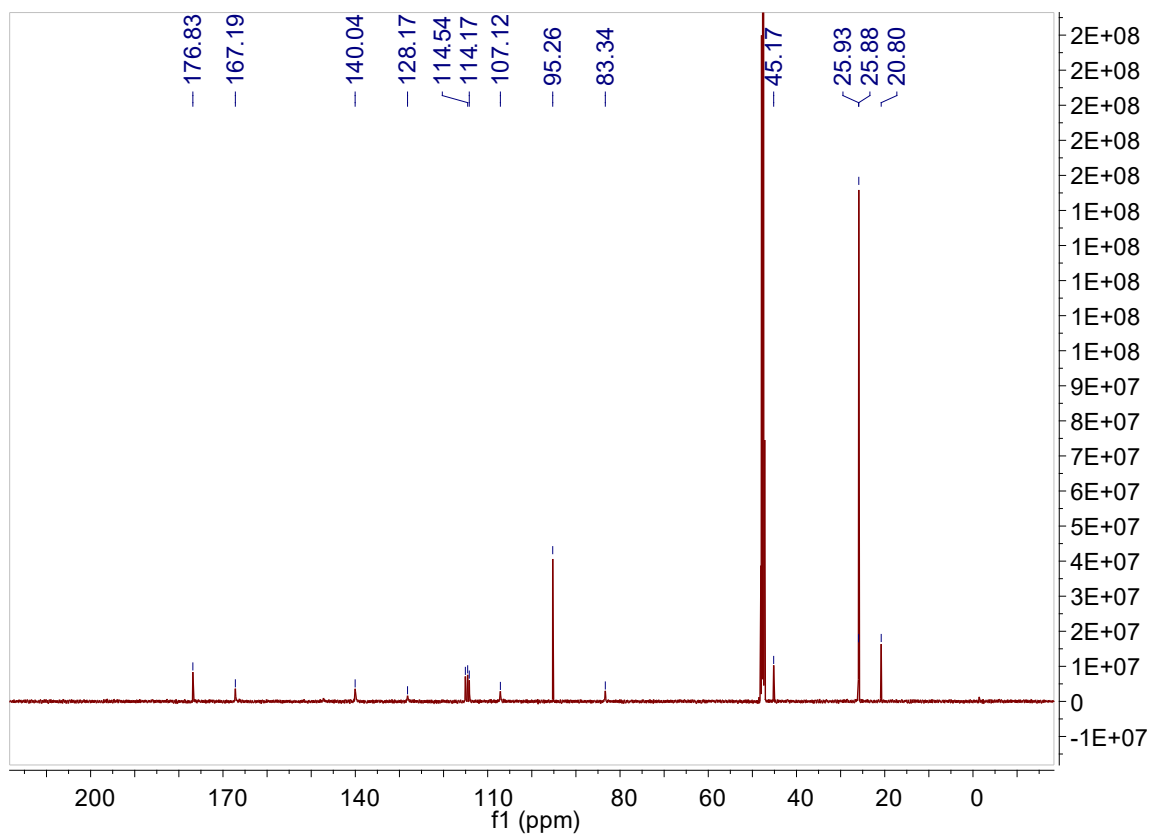


Figure S2. ^{13}C NMR spectrum of CFC-Cl.

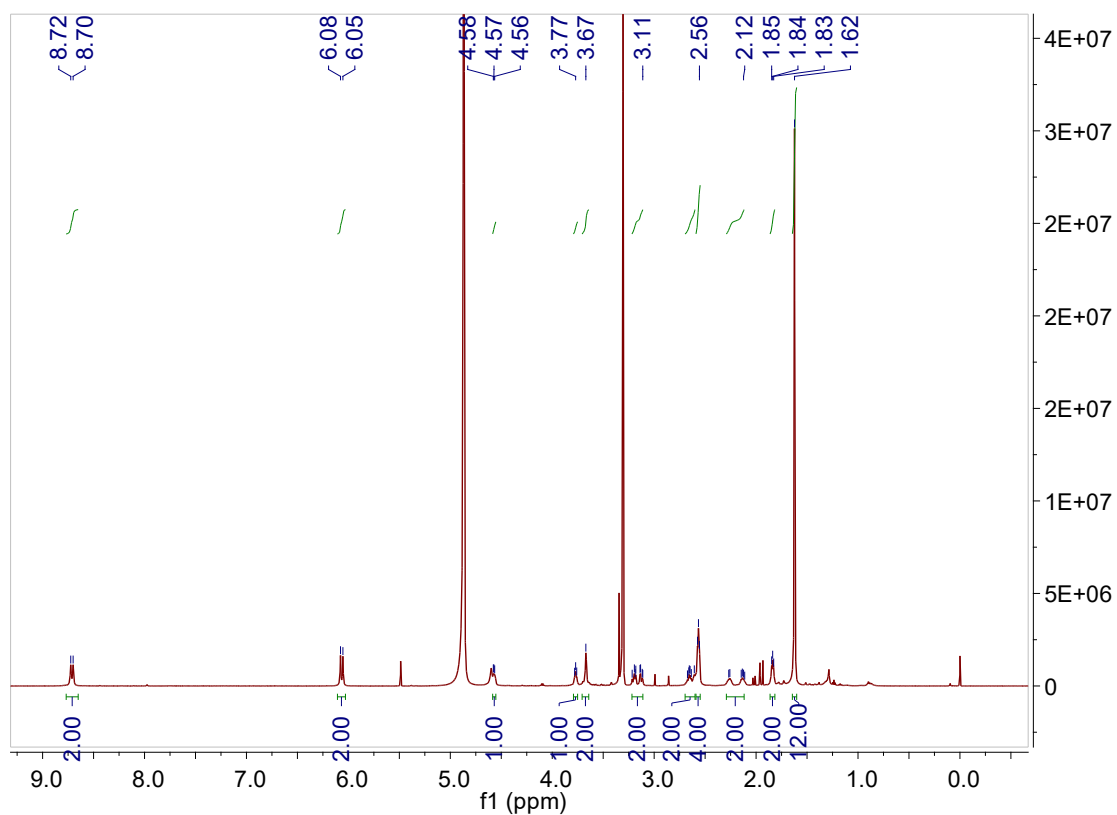


Figure S3. ^1H NMR spectrum of CFC-GSH.

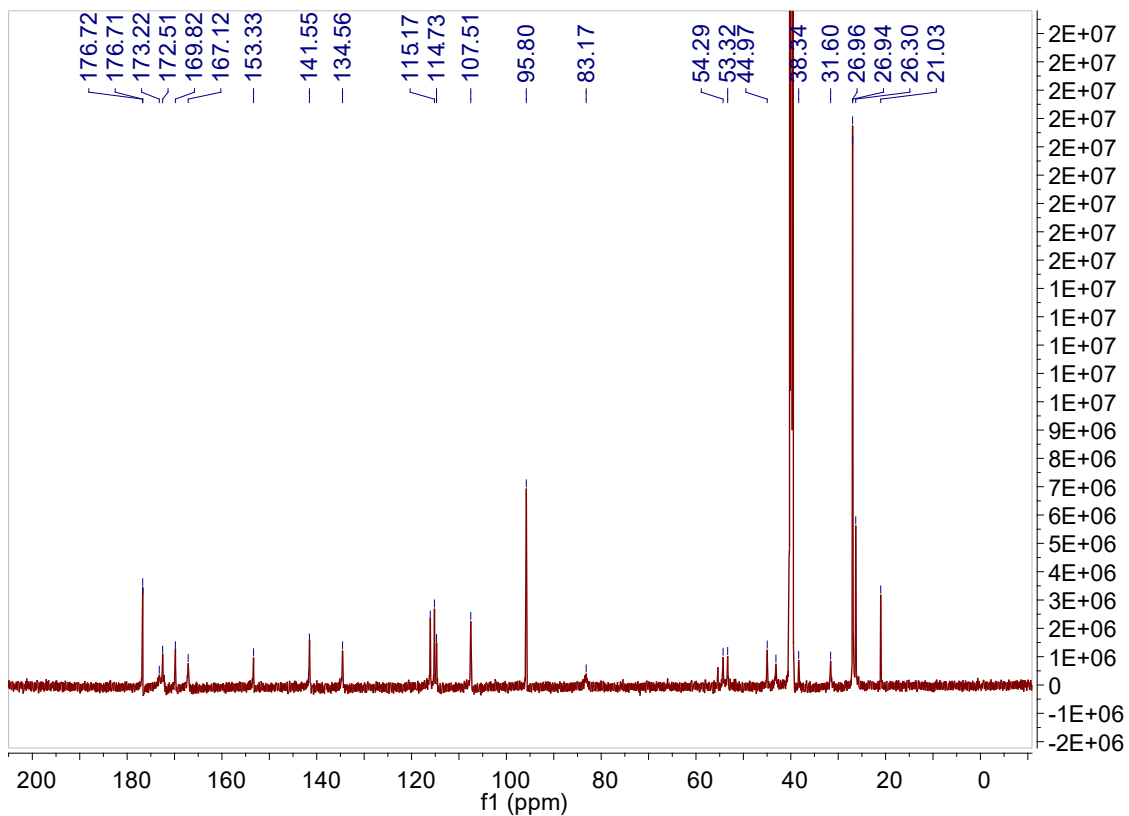


Figure S4. ^{13}C NMR spectrum of CFC-GSH.

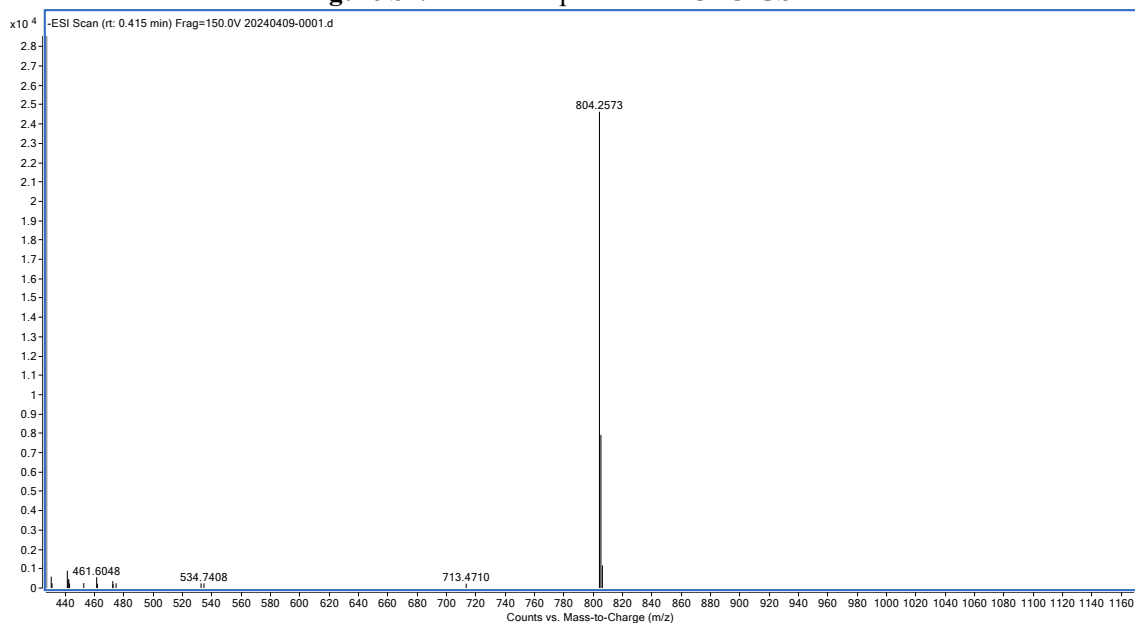


Figure S5. HRMS spectrum of CFC-GSH.

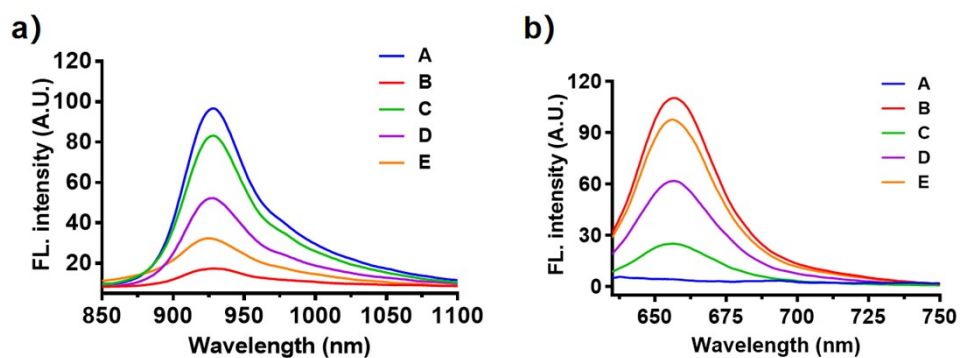


Figure S6. (a) NIR-II ($\lambda_{\text{ex}} = 808 \text{ nm}$), (b) NIR-I ($\lambda_{\text{ex}} = 620 \text{ nm}$) fluorescence spectra of CFC-GSH ($5 \mu\text{M}$) to (A) PBS, (B) GGT (80 U/L), (C) GGT (80 U/L) + acivicin (0.2 mM), (D) GGT (80 U/L) + acivicin (0.5 mM), (E) GGT (80 U/L) + acivicin (1 mM) at 37°C recorded at 22 min.

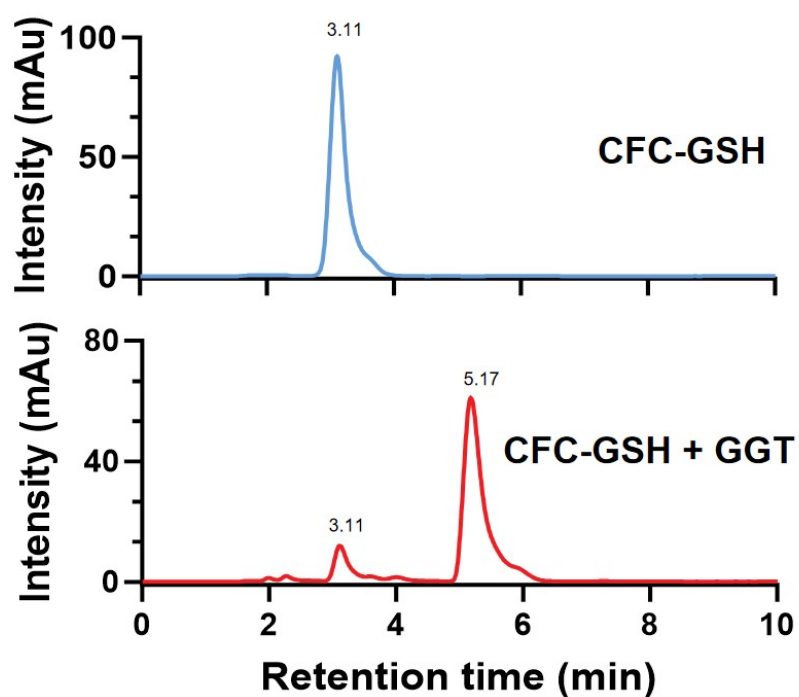


Figure S7. Verification of detection mechanism. HPLC spectra of CFC-GSH in the presence of GGT at 37°C .

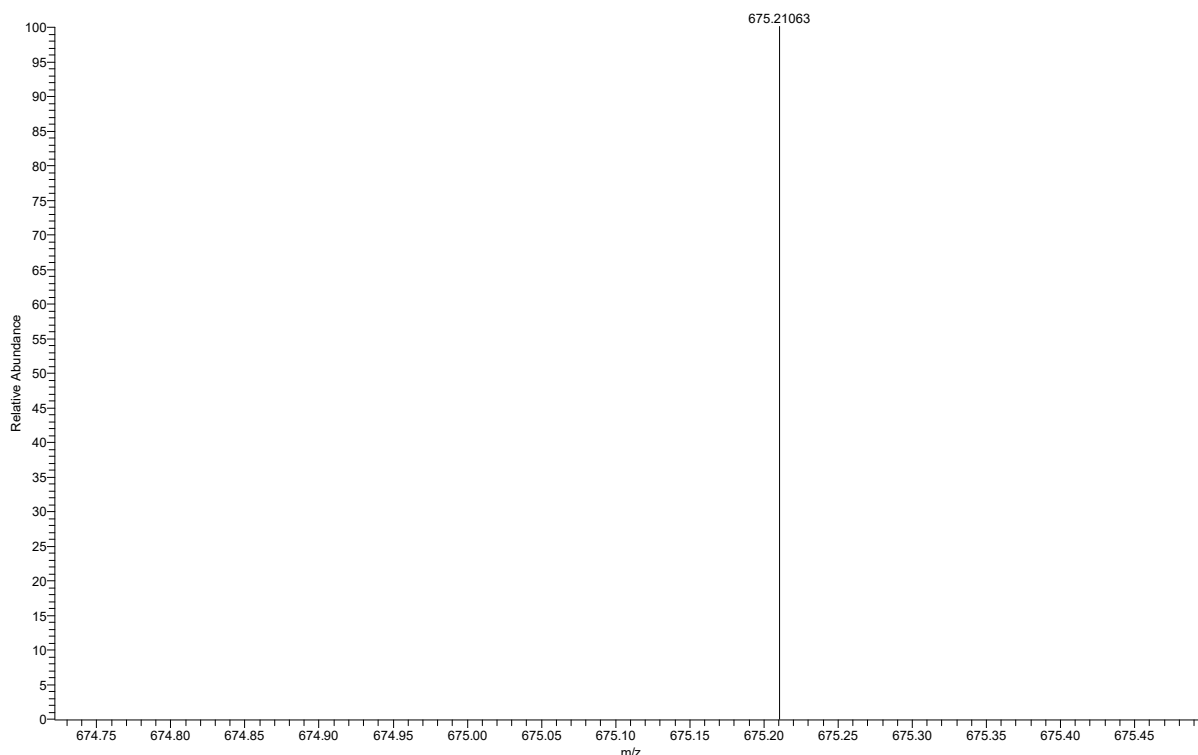


Figure S8. HRMS spectrum of **CFC-GSH** incubated with GGT at 37 °C for 22 min.

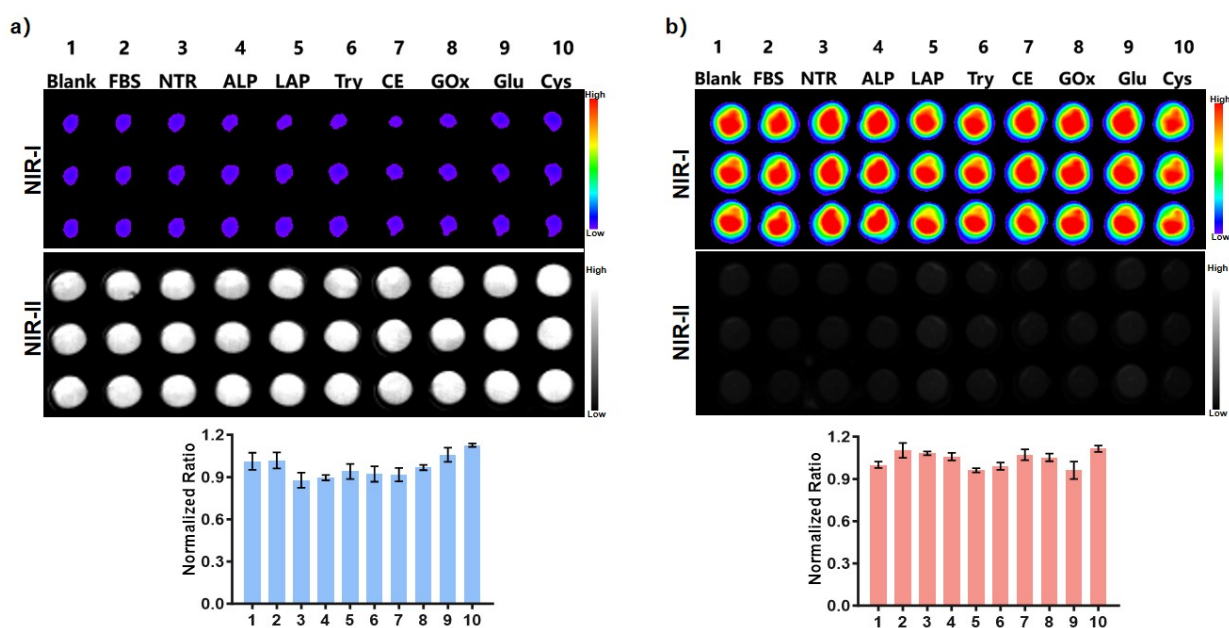


Figure S9. NIR-I ($\lambda_{\text{ex}} = 605 \text{ nm}$) and NIR-II ($\lambda_{\text{ex}} = 808 \text{ nm}$) fluorescent images with the corresponding quantitative analysis of the ratiometric fluorescence intensity of **CFC-GSH** ($5 \mu\text{M}$) toward potential biologically interfering substances in the absence (a) and presence (b) of GGT (80 U/L) at 37 °C for 22 min. Interfering substances: 1. blank, 2. 10% fetal bovine serum (FBS), 3. NTR, 4. ALP, 5. LAP, 6. Try, 7. CE, 8. GOx, 9. Glu, 10. Cys.

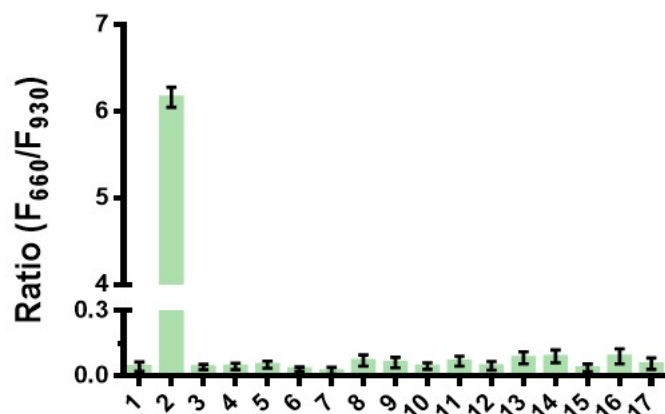


Figure S10. Fluorescence intensity ratio (F_{660}/F_{930}) of CFC-GSH (5 μ M) in the presence of other coexisting species at 37 °C for 22 min. Interfering substances: 1. blank, 2. GGT, 3. Hcy, 4. Iso, 5. Leu, 6. Arg, 7. Lys, 8. Phe, 9. Na⁺, 10. K⁺, 11. Mg²⁺, 12. Ca²⁺, 13. Al³⁺, 14. Fe²⁺, 15. H₂PO₄⁻, 16. NO₃⁻, 17. CO₃²⁻.

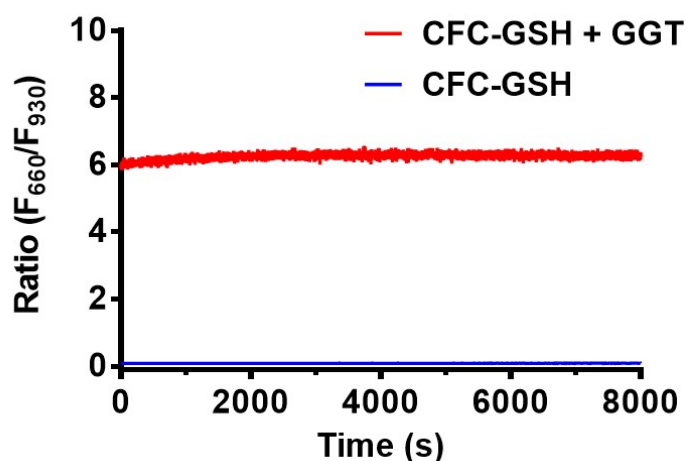


Figure S11. Photostability of fluorescence intensity ratio (F_{660}/F_{930}) of CFC-GSH (5 μ M) after incubation with/without GGT (80 U/L) for 22 min, respectively.

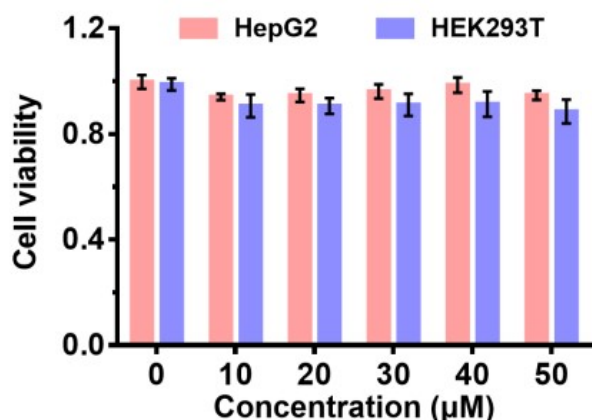


Figure S12. Cell viability of HepG2 cells (red) and HEK293T cells (blue) incubated with different concentrations of CFC-GSH (0–50 μ M) for 24 h.

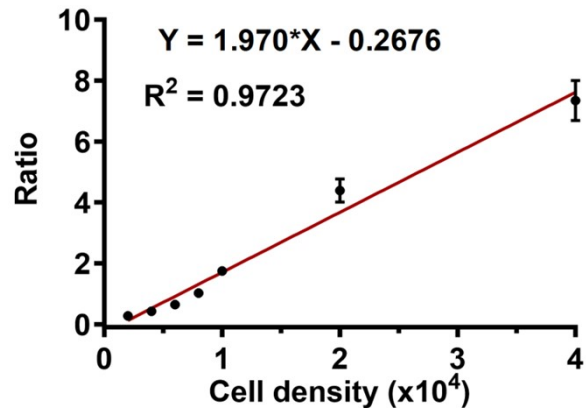


Figure S13. Linear relationship between the fluorescence intensity ratio (F_{660}/F_{930}) of CFC-GSH (5 μ M, 0.5% DMSO) and Hepa 1-6 cell density (2000, 4000, 6000, 8000, 10000, 20000, 40000).

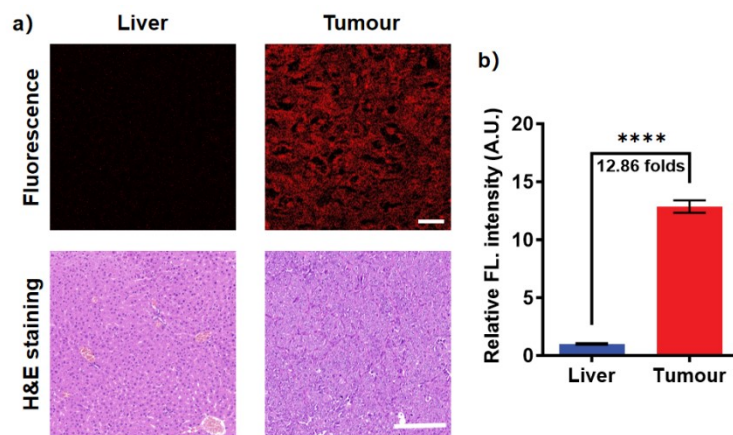
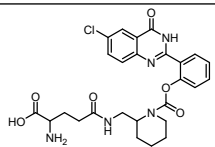
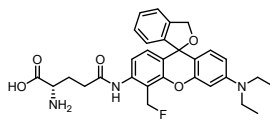
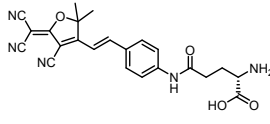
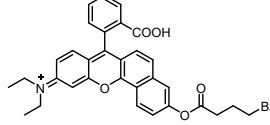
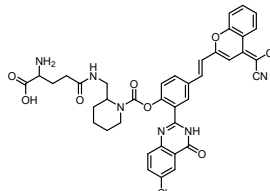
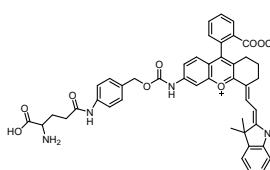
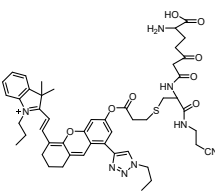
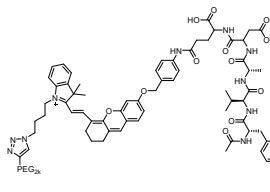
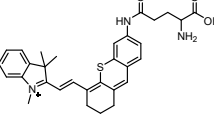


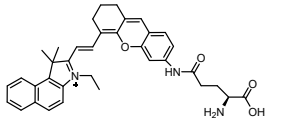
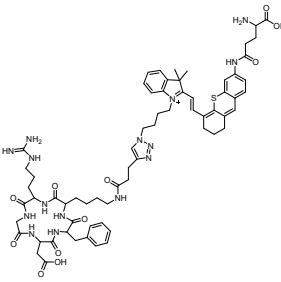
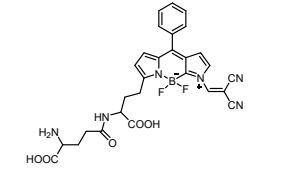
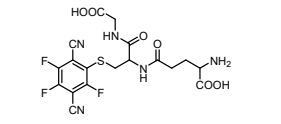
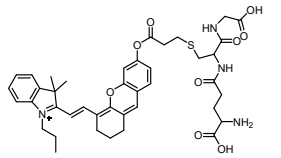
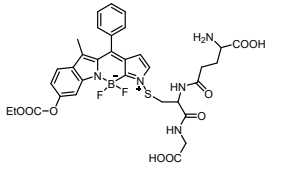
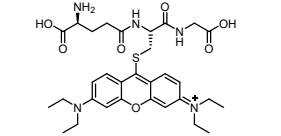
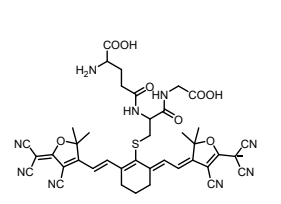
Figure S14. (a) Fluorescence confocal images (scale bar: 20 μ m) and H&E staining (scale bar: 200 μ m) of liver and tumour tissue harvested from the subcutaneous HCC-bearing mice after intertumoral injection CFC-GSH (50 μ L, 10 μ M in PBS, 1% DMSO) for 2 h. (b) Relative fluorescence intensity of CFC-GSH in (a).

Table S1. Comparison of the existing methods for detecting GGT.

Method	Signal	Procedure Complexity	Sensitivity	Tissue Penetration	Pros and Cons	Ref
Colorimetric analysis	Absorbance signal	Simple	Moderate	-	Simple, economical and rapid but limited in sensitivity and prone to interference from background signals.	[2]
High-performance liquid chromatography	Absorbance or fluorescence signal	Complex	High	-	High resolution and sensitivity, suitable for complex samples, but expensive and complicated operation.	[3]
Electrochemistry	Electrochemical current or potential signal	Moderate	High	-	Portable, real-time detection with high sensitivity, but susceptible to interference without optimized electrode design.	[4]
Optical detection and imaging	Fluorescent or luminescent signal	Simple	High	Regulable, near-infrared light penetrates deeper tissues	Outstanding sensitivity and broad applicability, enables in vivo imaging with high spatial resolution, but impacted by light scattering and poor light penetration at short-wavelength.	[5]
Positron emission tomography	Paired γ -photons	Complex	Extremely high	High	High sensitivity, enables in vivo imaging with high spatial resolution, but expensive, requires radioactive probe labeling, complex operation, radiation exposure risk.	[6]
Nuclear magnetic resonance imaging	Magnetic resonance signal	Moderate	Moderate	High	Radiation-free, high spatial resolution, suitable for long-term in vivo, but low sensitivity, weak signals and requires contrast agents	[7]

Table S2. Comparison of the proposed probe with other reported fluorescence probes for the detection of GGT.

Probe	Cleavage site	Working mode	λ_{ex} (nm)	λ_{em} (nm)	LOD (U/L)	Response time	Imaging application	Ref
	Glu	Turn-on	370	500	0.0167	25 min	HepG2 and HCT116 cells; tumour tissue	[8]
	Glu	Turn-on	533	576	-	-	SHIN3 cells; xenograft model mice	[9]
	Glu	Turn-on	560	610	0.014	26 min	NIH-3T3 and A2780 cells; zebrafish	[10]
	Glu	Turn-on	580	632	0.50	-	L02, HepG2 and LX-2 cells; zebrafish; acute injury and liver fibrotic model mice	[11]
	Glu	Turn-on	440	650	0.83	30 min	A2780 and OVCRA3 cells; fluorescence guiding surgery	[12]
	Glu	Turn-on	680	705	0.00518	-	HepG2 cells; fluorescence guiding surgery	[13]
	Glu	Turn-on	600	710	0.0012	-	HepG2 cells	[14]
	Glu	Turn-on	660	710	-	-	NIH-3T3 and 4T1 cells; xenograft model mice	[15]
	Glu	Turn-on	670	740	0.010	25 min	L02, HepG2 and LX-2 cells; xenograft model mice	[16]

	Glu	Turn-on	714	740	-	-	U87MG cells; xenograft model mice	[17]
	Glu	Turn-on	650/730	770	0.60	-	Normal and injured L02 cells; liver fibrosis mice	[18]
	Glu	Ratiometric	550/510	558/610	-	20 min	Gliomas tumour cells; xenograft model mice; tumour tissue	[19]
	GSH	Turn-on	405	490	0.117	-	OVCAR3 and SKOV3 cells	[20]
	GSH	Turn-on	590/660	708	0.50	18 min	Zebrafish	[21]
	GSH	Ratiometric	578/510	582/601	-	20 min	OVCAR5 and SKOV3 cells	[22]
	GSH	Ratiometric	593/445	620/545	0.010	17 min	SKOV3 and CAOV3 cells; tumour tissue; clinical specimens	[23]
	GSH	Ratiometric	890/650	930/660	0.04	22 min	HEK293T, NIH-3T3, Hepa 1-6, HepG2, SKOV3, A549 and B16F10 cells; xenograft model mice; metastasis tumour model mice; fluorescence angiography	This work

^a The ‘-’ represented the data could not be found.

Reference:

- [1] Chu F, Feng B, Liu M, Liu M, Chen F, Dong J, et al. A high-performance dual-modal probe boosted by pKa manipulation for colorimetric and fluorescent detection of hydrogen sulfide in living cells and food spoilage. *Dyes Pigments*. 2024; 222:111894-900.
- [2] Orłowski M, Meister A. γ -Glutamyl-p-nitroanilide: A new convenient substrate for determination and study of l- and d- γ -glutamyltranspeptidase activities. *Biochim Biophys Acta, Spec Sect Enzymol Subj*. 1963; 73(4):679-81.
- [3] Kiuchi K, Kiuchi K, Nagatsu T, Togari A, Kumagai H. Highly sensitive assay for γ -glutamyltranspeptidase activity by high-performance liquid chromatography with electrochemical detection. *J Chromatogr A*. 1986; 357:191-8.
- [4] Chen G, Ni S, Zhu S, Yang J, Yin Y. An electrochemical method to detect gamma glutamyl transpeptidase. *Int J Mol Sci*. 2012; 13(3):2801-9.
- [5] Zhang Y, Zhang Z, Wu M, Zhang R. Advances and perspectives of responsive probes for measuring γ -glutamyl transpeptidase. *ACS Meas Sci Au*. 2024; 4(1):54-75.
- [6] Ye S, Wang S, Gao D, Li K, Liu Q, Feng B, et al. A new γ -glutamyltranspeptidase-based intracellular self-assembly of fluorine-18 labeled probe for enhancing PET imaging in tumors. *Bioconjugate Chem*. 2020; 31(2):174-81.
- [7] Hai Z, Ni Y, Saimi D, Yang H, Tong H, Zhong K, et al. γ -Glutamyltranspeptidase-triggered intracellular gadolinium nanoparticle formation enhances the T2-weighted MR contrast of tumor. *Nano Lett*. 2019; 19(4):2428-33.
- [8] Ou-Yang J, Li Y-F, Wu P, Jiang W-L, Liu H-W, Li C-Y. Detecting and imaging of γ -glutamyltranspeptidase activity in serum, live cells, and pathological tissues with a high signal-stability probe by releasing a precipitating fluorochrome. *ACS Sensors*. 2018;3(7):1354-61.
- [9] Obara R, Kamiya M, Tanaka Y, Abe A, Kojima R, Kawaguchi T, et al. γ -Glutamyltranspeptidase (GGT)-activatable fluorescence probe for durable tumor imaging. *Angew Chem, Int Ed*. 2020;60(4):2125-9.
- [10] Li H, Yao Q, Xu F, Xu N, Duan R, Long S, et al. Imaging γ -Glutamyltranspeptidase for tumor identification and resection guidance via enzyme-triggered fluorescent probe. *Biomaterials*. 2018; 179:1-14.
- [11] Wang K, Wang W, Chen X-Y, Yang Y-S, Zhu H-L. Constructing a novel fluorescence detection method for γ -glutamyltranspeptidase and application on visualizing liver injury. *Biosens Bioelectron*. 2023; 219:114767-14.
- [12] Li K, Lyu Y, Huang Y, Xu S, Liu H-W, Chen L, et al. A de novo strategy to develop NIR precipitating

fluorochrome for long-term in situ cell membrane bioimaging. *Proc Natl Acad Sci U S A*. 2021; 118(8):e2018033118-e27.

[13] Liu Q, Yuan J, Jiang R, He L, Yang X, Yuan L, et al. γ -Glutamyltransferase-activatable fluoro-photoacoustic reporter for highly sensitive diagnosis of acute liver injury and tumor. *Anal Chem*. 2023; 95(3):2062-70.

[14] Zhang Y, Zhang G, Yang P, Moosa B, Khashab NM. Self-Immolative fluorescent and raman probe for real-time imaging and quantification of γ -glutamyl transpeptidase in living cells. *ACS Appl Mater Interfaces*. 2019; 11(31):27529-35.

[15] Wang X, He S, Cheng P, Pu K. A dual - locked tandem fluorescent probe for imaging of pyroptosis in cancer chemo - immunotherapy. *Adv Mater*. 2023; 35(10):2206510-8.

[16] Wang K, Chen X-Y, Zhang B, Yue Y, Wen X-L, Yang Y, et al. Near-infrared imaging of hepatocellular carcinoma and its medicinal treatment with a γ -glutamyl transpeptidase-monitoring fluorescence probe. *Biosens Bioelectron*. 2023; 241:115721-8.

[17] Zhou FY, Yang SK, Zhao C, Liu WW, Yao XF, Yu H, et al. γ -Glutamyl transpeptidase-activatable near-infrared nanoassembly for tumor fluorescence imaging-guided photothermal therapy. *Theranostics*. 2021; 11(14):7045-56.

[18] Miao M, Miao J, Zhang Y, Zhang J, She M, Zhao M, et al. An activatable near-infrared molecular reporter for fluoro-photoacoustic imaging of liver fibrosis. *Biosens Bioelectron*. 2023; 235:115399-405.

[19] Liu Y, Tan J, Zhang Y, Zhuang J, Ge M, Shi B, et al. Visualizing glioma margins by real-time tracking of γ -glutamyltranspeptidase activity. *Biomaterials*. 2018; 173:1-10.

[20] Huo R, Zheng X, Liu W, Zhang L, Wu J, Li F, et al. A two-photon fluorescent probe for sensitive detection and imaging of γ -glutamyl transpeptidase. *Chem Commun*. 2020; 56(74):10902-5.

[21] Li L, Shi W, Wu X, Gong Q, Li X, Ma H. Monitoring γ -glutamyl transpeptidase activity and evaluating its inhibitors by a water-soluble near-infrared fluorescent probe. *Biosens Bioelectron*. 2016; 81:395-400.

[22] Wang F, Zhu Y, Zhou L, Pan L, Cui Z, Fei Q, et al. Fluorescent in situ targeting probes for rapid imaging of ovarian - cancer - specific γ - glutamyltranspeptidase. *Angew Chem, Int Ed*. 2015; 54(25):7349-53.

[23] Zhou X, Liu Y, Liu Q, Yan L, Xue M, Yuan W, et al. Point-of-care ratiometric fluorescence imaging of tissue for the diagnosis of ovarian cancer. *Theranostics*. 2019; 9(16):4597-607.